PROCEEDINGS OF SCIENCE

Rare K- (*vs.*) B-decays

Ulrich Haisch[*†]
Institut für Theoretische Physik, Universität Zürich, CH-8057 Zürich, Switzerland
E-mail: uhaisch@physik.unizh.ch

We present a concise review of the recent theoretical progress concerning the standard model calculations of the rare $K_L \to \pi^0 \nu\bar{\nu}$, $K^+ \to \pi^+ \nu\bar{\nu}(\gamma)$, $\bar{B} \to X_s\gamma$, and $\bar{B} \to X_s\ell^+\ell^-$ decays. The current status and future of the model-independent analysis of rare K- and B-meson decays within constrained minimal-flavor-violation is also briefly discussed.

KAON International Conference
May 21-25 2007
Laboratori Nazionali di Frascati dell'INFN, Rome, Italy

[*]Speaker.

[†]We thank the organizers for the pleasant and stimulating atmosphere they were able to create during "KAON'07". Private communications with Einan Gardi and Mikołaj Misiak concerning $\bar{B} \to X_s\gamma$ are acknowledged. This work is supported by the Schweizer Nationalfonds.

PoS(KAON)056

1. Warm-up: basic facts about $s \to d\nu\bar{\nu}$ and $b \to s\gamma$

The $s \to d\nu\bar{\nu}$ transition is one of the rare examples of an electroweak (EW) process whose leading contribution starts at $O(G_F^2)$ within the standard model (SM). At the one-loop level it proceeds through Z-penguin and EW box diagrams which are highly sensitive to the underlying short-distance (SD) dynamics. Sample diagrams are shown on the left of Fig. 1. Separating the contributions according to the intermediate up-type quark running inside the loops, the QCD corrected amplitude takes the form

$$A_{\rm SM}(s \to d\nu\bar{\nu}) = \sum_{q=u,c,t} V_{qs}^* V_{qd} X_{\rm SM}^q \propto \frac{m_t^2}{M_W^2}(\lambda^5 + i\lambda^5) + \frac{m_c^2}{M_W^2}\ln\frac{m_c}{M_W}\lambda + \frac{\Lambda^2}{M_W^2}\lambda\,, \tag{1.1}$$

where V_{ij} denote the elements of the Cabibbo-Kobayashi-Maskawa (CKM) matrix and $\lambda = |V_{us}| = 0.225$. The hierarchy of the CKM elements would obviously favor the charm and up quark contributions, but the power-like Glashow-Iliopoulos-Maiani (GIM) mechanism, arising mainly from the $SU(2)_L$ breaking in the Z-penguin amplitude, leads to a very different picture. The top quark contribution, carrying a large CP-violating phase, accounts for $\sim 68\%$ of $A_{\rm SM}(s \to d\nu\bar{\nu})$, while corrections due to internal charm and up quarks amount to $\sim 29\%$ and a mere $\sim 3\%$. These properties imply that long-distance (LD) effects in the direct CP-violating $K_L \to \pi^0\nu\bar{\nu}$ mode are negligible, while they are highly suppressed in $K^+ \to \pi^+\nu\bar{\nu}(\gamma)$.

A related important feature, following from the EW structure of $A_{\rm SM}(s \to d\nu\bar{\nu})$ as well, is that the SD contributions to both $K \to \pi\nu\bar{\nu}$ decay modes are governed by a single effective operator, namely

$$Q_\nu = (\bar{s}_L\gamma_\mu d_L)(\bar{\nu}_L\gamma^\mu\nu_L)\,. \tag{1.2}$$

By virtue of the conservation of the $V-A$ current, large QCD logarithms appear only in the charm quark contribution to Eq. (1.1). The hadronic matrix element of Q_ν itself, can be extracted very precisely from the wealth of available data on $K \to \pi\ell\bar{\nu}$ ($K_{\ell 3}$) decays.

In summary, the superb theoretical cleanness and the enhanced sensitivity to both non-standard flavor and CP violation, make the $s \to d\nu\bar{\nu}$ channels unique tools to discover or, if no deviation is found, to set severe constraints on non-minimal-flavor-violating (MFV) physics where the hard GIM cancellation present in the SM and MFV is in general no longer active [1].

Unlike $s \to d\nu\bar{\nu}$, the $b \to s\gamma$ transition is dominated by perturbative QCD effects which replace the power-like GIM mechanism present in the EW vertex by a logarithmic one. The mild suppression of the QCD corrected SM amplitude

$$A_{\rm SM}(b \to s\gamma) = \sum_{q=u,c,t} V_{qb}^* V_{qs} K_{\rm SM}^q \propto \ln\frac{m_b}{M_W}\lambda^2 + \ln\frac{m_b}{M_W}\lambda^2 + \ln\frac{m_b}{M_W}\lambda^4\,, \tag{1.3}$$

reduces the sensitivity of the process to high scale physics, but enhances the $\bar{B} \to X_s\gamma$ branching ratio (BR) with respect to the purely EW prediction by a factor of around three. The logarithmic GIM cancellation originates from the non-conservation of the effective tensor operator

$$Q_7 = \frac{e}{16\pi^2} m_b(\bar{s}_L\sigma_\mu b_R)F^{\mu\nu}\,, \tag{1.4}$$

which is generated at the EW scale by photon penguin diagrams involving W-boson and top quark exchange. Sample one- and two-loop diagrams are shown on the right of Fig. 1.

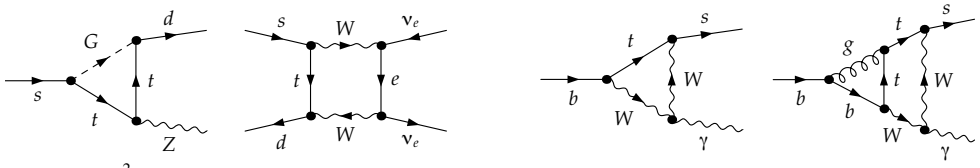

Figure 1: Feynman diagrams contributing to the $s \to d\nu\bar{\nu}$ (left) and $b \to s\gamma$ (right) transition in the SM. Their scaling behavior in the heavy top quark mass limit is also shown. See text for details.

After including logarithmic enhanced QCD effects, the dominant contribution to the partonic $b \to X_s^{\rm partonic}\gamma$ decay rate stems from charm quark loops that amount to $\sim 158\%$ of $A_{\rm SM}(b \to s\gamma)$. The top contribution is with $\sim -60\%$ of $A_{\rm SM}(b \to s\gamma)$ compared to the charm quark effects less than half as big and has the opposite sign. Diagrams involving up quarks are suppressed by small CKM factors and lead to an effect of only $\sim 2\%$ in $A_{\rm SM}(b \to s\gamma)$. Due to the inclusive character of the $\bar{B} \to X_s\gamma$ mode and the heaviness of the bottom quark, $m_b \gg \Lambda \sim \Lambda_{\rm QCD}$, non-perturbative effects arise only as small corrections to the partonic decay rate.

In summary, the good theoretical control on and experimental accessibility of the $b \to s\gamma$ rate, and its large generic sensitivity to non-standard sources of flavor and *CP* violation, allows to derive stringent constraints on a variety of new physics (NP) models, in particular on those where the flavor-violating chiral transition of the amplitude is not suppressed.

2. Recent theoretical progress in $K_L \to \pi^0\nu\bar{\nu}$ and $K^+ \to \pi^+\nu\bar{\nu}(\gamma)$

After summation over the three lepton families the SM BRs of the $K \to \pi\nu\bar{\nu}$ modes read

$$\mathrm{BR}(K_L \to \pi^0\nu\bar{\nu})_{\rm SM} = \kappa_L \left(\frac{\mathrm{Im}\,\lambda_t}{\lambda^5} X\right)^2, \tag{2.1}$$

$$\mathrm{BR}(K^+ \to \pi^+\nu\bar{\nu}(\gamma))_{\rm SM} = \kappa_+(1+\Delta_{\rm EM}) \left[\left(\frac{\mathrm{Im}\,\lambda_t}{\lambda^5} X\right)^2 + \left(\frac{\mathrm{Re}\,\lambda_t}{\lambda^5} X + \frac{\mathrm{Re}\lambda_c}{\lambda}\left(P_c + \delta P_{c,u}\right)\right)^2\right], \tag{2.2}$$

where $\lambda_i = V_{is}^* V_{id}$. The top quark contribution $X = 1.456 \pm 0.017_{m_t} \pm 0.013_{\mu_t} \pm 0.015_{\rm EW}$ is known through next-to-leading order (NLO) in QCD [2]. Its overall uncertainty of $\sim 2\%$ is in equal shares due to the parametric error on the top quark mass, the sensitivity on the matching scale μ_t, and two-loop EW effects for which only the leading term in the heavy top quark mass expansion has been calculated [3].

Major theoretical progress has been recently made concerning the extraction of the hadronic $\langle \pi^i | \bar{s}\gamma_\mu d | K^j \rangle$ matrix elements from $K_{\ell 3}$ data, by extending the classic chiral perturbation theory (ChPT) analysis of leading order (LO) $O(p^2\varepsilon^{(2)})$ isospin-breaking effects [4]. Here $\varepsilon^{(2)} \propto (m_u - m_d)/m_s$. The inclusion of NLO $O(p^4\varepsilon^{(2)})$ and partial next-to-next-to-leading order (NNLO) $O(p^6\varepsilon^{(2)})$ corrections in the ChPT expansion [5] leads to a reduction of the uncertainties on the $K_L \to \pi^0\nu\bar{\nu}$ and $K^+ \to \pi^+\nu\bar{\nu}$ matrix elements by a factor of ~ 4 and ~ 7. Since the overall uncertainties on $\kappa_L = (2.229 \pm 0.017) \times 10^{-10}\,(\lambda/0.225)^8$ and $\kappa_+ = (5.168 \pm 0.025) \times 10^{-10}\,(\lambda/0.225)^8$

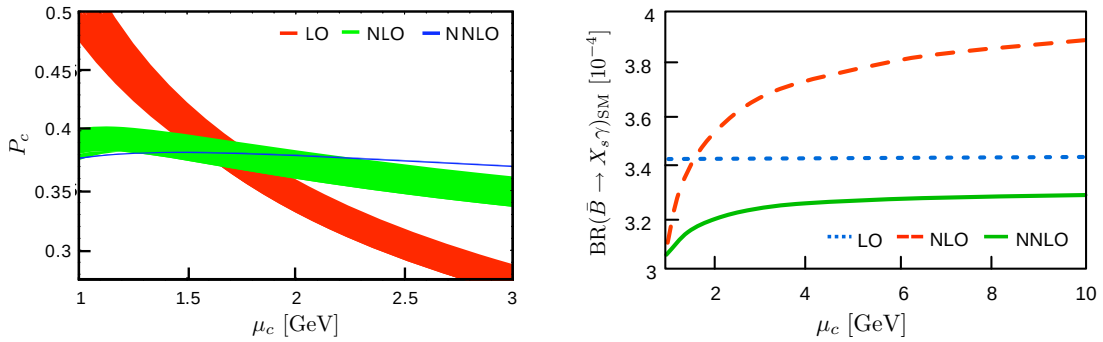

Figure 2: Charm quark mass renormalization scale μ_c dependence of P_c (left) and $\mathrm{BR}(\bar{B} \to X_s\gamma)_{\mathrm{SM}}$ (right) at LO, NLO, and NNLO in QCD. The width of the curves on the left indicate the uncertainty due to higher order terms in α_s that affect the evaluation of $\alpha_s(\mu_c)$ from $\alpha_s(M_Z)$. See text for details.

[5] are now dominated by experimental errors, a further improvement in the extraction of the rare K-decay matrix elements will be possible with improved data for the $K_{\ell 3}$ slopes and $K^+_{\ell 3}$ BRs. LD QED corrections affecting $K^+ \to \pi^+ \nu\bar{\nu}(\gamma)$ are encoded by Δ_{EM} in Eq. (2.2). At LO in the ChPT expansion, these infrared finite $O(p^2\alpha)$ corrections amount to $\Delta_{\mathrm{EM}} = -0.003$ [5] for a maximum energy of 20 MeV of the undetected photon. More details on the ChPT analysis of rare K-decay matrix elements can be found in [5].

The parameter P_c entering Eq. (2.2) results from Z-penguin and EW box diagrams involving internal charm quark exchange. As now both high- and low-energy scales are involved, a complete renormalization group analysis of this term is required. In this manner, large logarithms $\ln m_c/M_W$ are resummed to all orders in α_s. The inclusion of NNLO QCD corrections [6] leads to a significant reduction of the theoretical uncertainty by a factor of ~ 4, as it removes almost the entire sensitivities of P_c on the charm quark mass renormalization scale μ_c and on higher order terms in α_s that affect the evaluation of $\alpha_s(\mu_c)$ from $\alpha_s(M_Z)$. This is illustrated by the plot in the left panel of Fig. 2. For $m_c = (1.30 \pm 0.05)\,\mathrm{GeV}$ one obtains the NNLO value $P_c = (0.374 \pm 0.031_{m_c} \pm 0.009_{\mathrm{pert}} \pm 0.009_{\alpha_s})\,(0.225/\lambda)^4$ [6], where the individual errors are due to the uncertainty on the charm quark $\overline{\mathrm{MS}}$ mass, higher-order perturbative effects, and the parametric error on $\alpha_s(M_Z)$. Since the residual error on P_c is now fully dominated by the parametric uncertainty coming from m_c, a better determination of the charm quark mass is clearly an important theoretical goal in connection with $K^+ \to \pi^+ \nu\bar{\nu}(\gamma)$.

To gain an accuracy on the $K^+ \to \pi^+ \nu\bar{\nu}(\gamma)$ BR of a few percent, it is necessary to account for subleading effects not described by the effective Hamiltonian that includes the dimension-six operator Q_ν of Eq. (1.2). The subleading corrections can be divided into two groups: *i*) contributions of dimension-eight four fermion operators generated at the charm quark mass renormalization scale μ_c [7, 8], and *ii*) genuine LD contributions due to up quark loops which can be described within the framework of ChPT [8]. Both contributions can be effectively included by $\delta P_{c,u} = 0.04 \pm 0.02$ [8] in Eq. (2.2). Numerically, they lead to an enhancement of $\mathrm{BR}(K^+ \to \pi^+ \nu\bar{\nu}(\gamma))_{\mathrm{SM}}$ by $\sim 7\%$. The quoted residual error of $\delta P_{c,u}$ could in principle be reduced by means of a dedicated lattice QCD computation [9].

Taking into account all the indirect constraints from the latest unitarity triangle fit [10], one

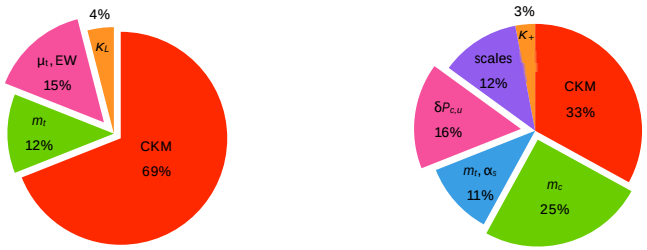

Figure 3: Error budget of the SM prediction of $\mathrm{BR}(K_L \to \pi^0 \nu\bar{\nu})$ (left) and $\mathrm{BR}(K^+ \to \pi^+ \nu\bar{\nu}(\gamma))$ (right). See text for details.

finds, by adding errors quadratically, the following SM predictions for the two $K \to \pi\nu\bar{\nu}$ rates

$$\mathrm{BR}(K_L \to \pi^0 \nu\bar{\nu})_{\mathrm{SM}} = (2.54 \pm 0.35) \times 10^{-11}\,, \tag{2.3}$$

$$\mathrm{BR}(K^+ \to \pi^+ \nu\bar{\nu}(\gamma))_{\mathrm{SM}} = (7.96 \pm 0.86) \times 10^{-11}\,. \tag{2.4}$$

The error budgets of the SM predictions of both $K \to \pi\nu\bar{\nu}$ decays are illustrated by the pie charts in Fig. 3. As the breakdown of the residual uncertainties shows, both decay modes are at present subject mainly to parametric errors (81%, 69%) stemming from the CKM parameters, the quark masses m_c and m_t, and $\alpha_s(M_Z)$. The non-parametric errors in $K_L \to \pi^0 \nu\bar{\nu}$ are dominated by the uncertainty due to higher-order perturbative effects (15%), while in the case of $K^+ \to \pi^+ \nu\bar{\nu}(\gamma)$ the errors due to dimension-eight charm and LD up quark effects (16%) and left over scale uncertainties (12%) are similar in size. Given the expected improvement in the extraction of the CKM elements through the B-factories, SM predictions for both $K \to \pi\nu\bar{\nu}$ rates with an accuracy significantly below 10% should be possible before the end of this decade. Such precisions are unique in the field of flavor-changing-neutral-current processes.

3. Recent theoretical progress in $\bar{B} \to X_s\gamma$ and $\bar{B} \to X_s\ell^+\ell^-$

Considerable effort has gone into the calculation of fixed-order logarithmic enhanced NNLO QCD corrections to $\bar{B} \to X_s\gamma$ [11, 12, 13, 14]. A crucial part of the NNLO calculation is the interpolation in the charm quark mass performed in [13]. The three-loop $O(\alpha_s^2)$ matrix elements of the current-current operators $Q_{1,2}$ contain the charm quark, and the NNLO calculation of these matrix elements is essential to reduce the overall theoretical uncertainty of the SM calculation. In fact, the largest part of the theoretical uncertainty in the NLO analysis of the BR is related to the definition of the mass of the charm quark [15] that enters the $O(\alpha_s)$ matrix elements $\langle s\gamma|Q_{1,2}|b\rangle$. The latter matrix elements are non-vanishing at two loops only and the scale at which m_c should be normalized is therefore undetermined at NLO. Since varying m_c between $m_c(m_c) \sim 1.25\,\mathrm{GeV}$ and $m_c(m_b) \sim 0.85\,\mathrm{GeV}$ leads to a shift in the NLO BR of more than 10% this issue is not an academic one.

Finding the complete NNLO correction to $\langle s\gamma|Q_{1,2}|b\rangle$ is a formidable task, since it involves the evaluation of hundreds of three-loop on-shell vertex diagrams that are presently not even known in the case $m_c = 0$. The approximation made in [13] is based on the observation that at the physical point $m_c \sim 0.25\,m_b$ the large $m_c \gg m_b$ asymptotic form of the exact $O(\alpha_s)$ [16] and large-β_0

$O(\alpha_s^2\beta_0)$ [12] result matches the small $m_c \ll m_b$ expansion rather well. This feature prompted the analytic calculation of the leading term in the $m_c \gg m_b$ expansion of the three-loop diagrams, and to use the obtained information to perform an interpolation to smaller values of m_c assuming the $O(\alpha_s^2\beta_0)$ part to be a good approximation of the full $O(\alpha_s^2)$ result for vanishing charm quark mass. The uncertainty related to this procedure has been assessed in [13] by employing three ansätze with different boundary conditions at $m_c = 0$. A complete calculation of the $O(\alpha_s^2)$ corrections to $\langle s\gamma|Q_{1,2}|b\rangle$ in the latter limit or, if possible, for $m_c \sim 0.25\, m_b$, would resolve this ambiguity and should therefore be attempted.

Combining the aforementioned results it was possible to obtain the first theoretical estimate of the total BR of $\bar{B} \to X_s\gamma$ at NNLO. For a photon energy cut of $E_\gamma > E_{\rm cut}$ with $E_{\rm cut} = 1.6\,\text{GeV}$ in the $\bar{B}$-meson rest-frame the improved SM evaluation is given by [13, 14]

$$\text{BR}(\bar{B} \to X_s\gamma)_{\rm SM} = (3.15 \pm 0.23) \times 10^{-4}\,, \tag{3.1}$$

where the uncertainties from hadronic power corrections (5%), parametric dependences (3%), higher-order perturbative effects (3%), and the interpolation in the charm quark mass (3%) have been added in quadrature to obtain the total error.

The reduction of the renormalization scale dependence at NNLO is clearly seen in the right panel of Fig. 2. The most pronounced effect occurs in the case of μ_c that was the main source of uncertainty at NLO. The current uncertainty of 3% due to higher-order effects is estimated from the variations of the NNLO estimate under change of renormalization scales. The central value in Eq. (3.1) corresponds to the choice $\mu_{W,b,c} = (160, 2.5, 1.5)\,\text{GeV}$. More details on the phenomenological analysis including the list of input parameters can be found in [13].

It is well-known that the operator product expansion (OPE) for $\bar{B} \to X_s\gamma$ has certain limitations which stem from the fact that the photon has a partonic substructure. In particular, the local expansion does not apply to contributions from operators other than Q_7, in which the photon couples to light quarks [17, 18]. While the presence of non-local power corrections was thus foreseen such terms have been studied until recently only in the case of the (Q_8, Q_8) interference [17]. In [19] the analysis of non-perturbative effects that go beyond the local OPE have been extended to the enhanced non-local terms emerging from (Q_7, Q_8) insertions. The found correction scales like $O(\alpha_s\Lambda/m_b)$ and its effect on the BR was estimated using the vacuum insertion approximation to be $-[0.3, 3.0]\%$. A measurement of the flavor asymmetry between $\bar{B}^0 \to X_s\gamma$ and $B^- \to X_s\gamma$ could help to sustain this numerical estimate [19]. Potentially as important as the latter corrections are those arising from the $(Q_{1,2}, Q_7)$ interference. Naive dimensional analysis suggests that some non-perturbative corrections to them also scale like $O(\alpha_s\Lambda/m_b)$. Since at the moment there is not even an estimate of those corrections, a non-perturbative uncertainty of 5% has been assigned to the result in Eq. (3.1). This error is the dominant theoretical uncertainty at present and thought to include all known [19] and unknown $O(\alpha_s\Lambda/m_b)$ terms. Calculating the precise impact of the enhanced non-local power corrections may remain notoriously difficult given the limited control over non-perturbative effects on the light cone.

A further complication in the calculation of $\bar{B} \to X_s\gamma$ arises from the fact that all measurements impose stringent cuts on the photon energy to suppress the background from other B-meson decay processes. Restricting E_γ to be close to the physical endpoint $E_{\rm max} = m_B/2$, leads to a breakdown of the local OPE, which can be cured by resummation of an infinite set of leading-twist terms

into a non-perturbative shape function [20]. A detailed knowledge of the shape function and other subleading effects is required to extrapolate the measurements to a region where the conventional OPE can be trusted.

The transition from the shape function to the OPE region can be described by a multi-scale OPE (MSOPE) [21]. In addition to the hard scale $\mu_h \sim m_b \sim 5\,\text{GeV}$, this expansion involves a hard-collinear scale $\mu_{hc} \sim \sqrt{m_b \Delta} \sim 2.5\,\text{GeV}$ corresponding to the typical hadronic invariant mass of the final state X_s, and a soft scale $\mu_s \sim \Delta \sim 1.5\,\text{GeV}$ related to the width $\Delta/2 = m_b/2 - E_{\text{cut}}$ of the energy window in which the photon spectrum is measured. In the MSOPE framework, the perturbative tail of the spectrum receives calculable corrections at all three scales, and may be subject to large perturbative corrections due to the presence of terms proportional to $\alpha_s(\sqrt{m_b\Delta}) \sim 0.27$ and $\alpha_s(\Delta) \sim 0.36$.

A systematic MSOPE analysis of the (Q_7, Q_7) interference at NNLO has been performed in [22]. Besides the hard matching corrections, it involves the two-loop logarithmic and constant terms of the jet [21, 24] and soft function [25]. The three-loop anomalous dimension of the shape function remains unknown and is not included. The MSOPE result can be combined with the fixed-order prediction by computing the fraction of events $1-T$ that lies in the range $E_{\text{cut}} = [1.0, 1.6]\,\text{GeV}$. The analysis [22] yields

$$1 - T = 0.07^{+0.03}_{-0.05\,\text{pert}} \pm 0.02_{\text{hadr}} \pm 0.02_{\text{pars}}\,, \tag{3.2}$$

where the individual errors are perturbative, hadronic, and parametric. The quoted value is almost twice as large as the NNLO estimate $1 - T = 0.04 \pm 0.01_{\text{pert}}$ obtained in fixed-order perturbation theory [13, 14, 23] and plagued by a significant additional theoretical error related to low-scale perturbative corrections. These large residual scale uncertainties indicate a slow convergence of the MSOPE series expansion in the tail region of the photon energy spectrum. Given that Δ is always larger than 1.4 GeV and thus fully in the perturbative regime this feature is unexpected.

Additional theoretical information on the shape of the photon energy spectrum can be obtained from the universality of soft and collinear gluon radiation. Such an approach can be used to predict large logarithms of the form $\ln(E_{\text{max}} - E_{\text{cut}})$. These computations have also achieved NNLO accuracy [26] and incorporate Sudakov and renormalon resummation via dressed gluon exponentiation (DGE) [26, 27]. The present NNLO estimate of $1 - T = 0.016 \pm 0.003_{\text{pert}}$ [26, 28] indicates a much thinner tail of the photon energy spectrum and a considerable smaller perturbative uncertainty than reported in [22]. The DGE analysis thus supports the view that the integrated photon energy spectrum below $E_{\text{cut}} = 1.6\,\text{GeV}$ is well approximated by a fixed-order perturbative calculation, complemented by local OPE power corrections. To understand how precisely the tail of the photon energy spectrum can be calculated requires nevertheless further theoretical investigations.

The study of $b \to s\ell^+\ell^-$ transitions can yield useful complementary information, when confronted with the less rare $b \to s\gamma$ decays, in testing the flavor sector of the SM. In particular, a precise measurement of the inclusive $\bar{B} \to X_s\ell^+\ell^-$ decay distributions would be welcome in view of NP searches, because they are amenable to clean theoretical descriptions for dilepton invariant masses in the ranges $1\,\text{GeV}^2 < q^2 < 6\,\text{GeV}^2$ [29, 30, 31] and $q^2 > 14\,\text{GeV}^2$ [32].

The SM calculations of the differential rate and forward-backward (FB) asymmetry have both reached NNLO precision [29, 30, 33]. In the case of the the dilepton invariant mass spectrum,

integrated over the low-q^2 region, the most recent SM prediction reads [31]

$$\mathrm{BR}(\bar{B}\to X_s\ell^+\ell^-)_{\mathrm{SM}}^{1\,\mathrm{GeV}^2<q^2<6\,\mathrm{GeV}^2}=(1.59\pm0.11)\times10^{-6}\,. \tag{3.3}$$

The position of the zero of the FB asymmetry is known to be especially sensitive to NP effects. In the SM one finds [30]

$$q^2_{0,\mathrm{SM}}=(3.76\pm0.33)\,\mathrm{GeV}^2\,. \tag{3.4}$$

The total errors in Eqs. (3.3) and (3.4) have been obtained by adding the individual parametric and perturbative uncertainties in quadrature. Besides the differential rate and FB asymmetry, an angular decomposition of $\bar{B}\to X_s\ell^+\ell^-$ provides a third observable that is sensitive to a different combination of Wilson coefficients. This recent observation [36] might allow to extract SD information from limited data on $\bar{B}\to X_s\ell^+\ell^-$ in the low-q^2 region more efficiently.

Like in the case of $\bar{B}\to X_s\gamma$, experimental cuts complicate the theoretical description of $\bar{B}\to X_s\ell^+\ell^-$ as they make the measured decay distributions sensitive to the non-perturbative shape function [34]. In particular, putting an upper cut $M_{X_s}^{\mathrm{cut}}=[1.8,2.0]\,\mathrm{GeV}$ on the hadronic invariant mass of X_s [35], in order to suppress the background from $\bar{B}\to X_c\ell\bar{\nu}\to X_s\ell^+\ell^-\nu\bar{\nu}$ at small q^2, causes a reduction of the rate by $(10-30)\%$ [34]. Although the reduction can be accurately calculated using the universal $\bar{B}\to X_s\gamma$ shape function [34], subleading shape functions may introduce an additional error of 5% in Eq. (3.3). Similarly, no additional uncertainty for unknown subleading non-perturbative corrections has been included in Eqs. (3.3) and (3.4). Most importantly, uncalculated $O(\alpha_s\Lambda/m_b)$ non-perturbative corrections may imply an additional uncertainty of 5% in the above formulas. This issue deserves an dedicated study.

4. CMFV: combining $K^+\to\pi^+\nu\bar{\nu}(\gamma)$, $\bar{B}\to X_s\gamma$, $\bar{B}\to X_s\ell^+\ell^-$, and $Z\to b\bar{b}$

A way to study possible NP effects in flavor physics consists in constraining the Wilson coefficients of the operators in the low-energy effective theory. This model-independent approach to MFV has been applied combining various K- and B-meson decay modes both including [37] and neglecting [38, 39, 40] operators that do not contribute in the SM, that is, so-called constrained MFV (CMFV) [41] scenarios.

The main goal of the recent CMFV study [40] was an improved determination of the range allowed for the NP contribution $\Delta C=C-C_{\mathrm{SM}}$ to the universal Z-penguin by a thorough global fit to the $Z\to b\bar{b}$ pseudo observables (POs) R_b^0, A_b, and $A_{\mathrm{FB}}^{0,b}$ [42] and the measured $\bar{B}\to X_s\gamma$ [43] and $\bar{B}\to X_s\ell^+\ell^-$ [35] rates. The derived model-independent bounds

$$\Delta C=-0.026\pm0.264\ \ (68\%\,\mathrm{CL})\,,\qquad \Delta C=[-0.483,0.368]\ \ (95\%\,\mathrm{CL})\,, \tag{4.1}$$

imply that large negative contributions that would reverse the sign of the SM Z-penguin amplitude are highly disfavored in CMFV scenarios due to the strong constraint from R_b^0 [40]. Interestingly, such a conclusion cannot be drawn by considering only flavor constraints [39], since a combination of $\mathrm{BR}(\bar{B}\to X_s\gamma)$, $\mathrm{BR}(\bar{B}\to X_s\ell^+\ell^-)$, and $\mathrm{BR}(K^+\to\pi^+\nu\bar{\nu}(\gamma))$ does not allow to distinguish the SM solution $\Delta C=0$ from the wrong-sign case $\Delta C\sim-2$ at present. The constraint on ΔC within CMFV following from the simultaneous use of R_b^0, A_b, $A_{\mathrm{FB}}^{0,b}$, $\mathrm{BR}(\bar{B}\to X_s\gamma)$, and $\mathrm{BR}(\bar{B}\to X_s\ell^+\ell^-)$ can be seen in the left panel of Fig. 4.

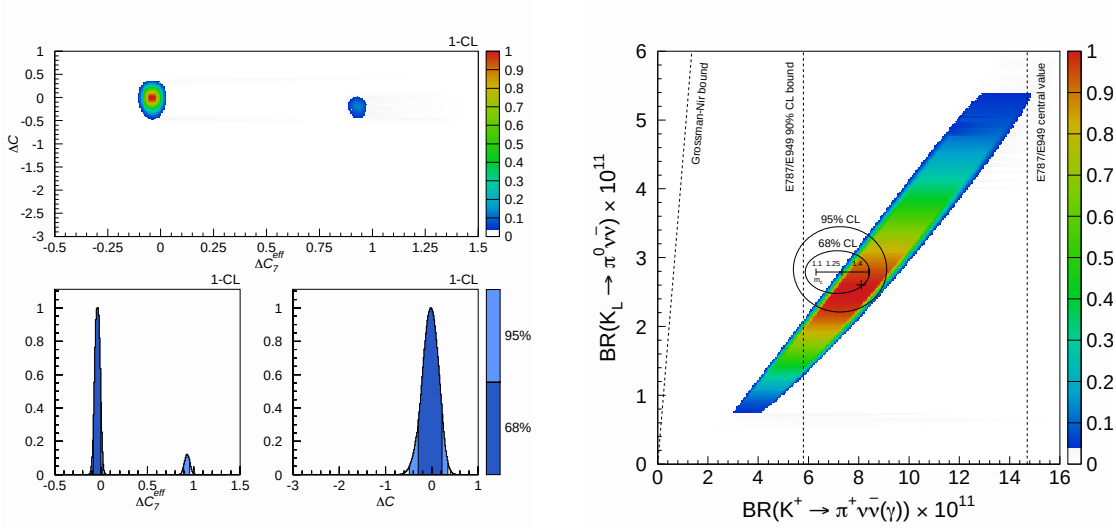

Figure 4: Left: Constraints on $\Delta C_7^{\rm eff}$ and ΔC within CMFV that follow from a combination of the measurements of $\bar{B} \to X_s\gamma$, $\bar{B} \to X_s\ell^+\ell^-$, and $Z \to b\bar{b}$. The colors encode the frequentist $1-$CL level and the corresponding 68% CL and 95% CL regions as indicated by the bars on the right side of the panel. Right: Frequentist $1-$CL level of $\mathrm{BR}(K^+ \to \pi^+\nu\bar{\nu}(\gamma))$ *vs.* $\mathrm{BR}(K_L \to \pi^0\nu\bar{\nu})$ in CMFV. The two black ellipses indicate the 68% CL and 95% CL regions in the SM while the best fit value within CMFV is specified by the black cross. The central value of $\mathrm{BR}(K^+ \to \pi^+\nu\bar{\nu}(\gamma))_{\rm SM}$ as a function of the charm quark $\overline{\rm MS}$ mass in GeV and the lower experimental 90% CL bound and central value are also shown. See text for details.

One can also infer from this figure that two regions, resembling the two possible signs of the amplitude $A(b \to s\gamma) \propto C_7^{\rm eff}(m_b)$, satisfy all existing experimental bounds. The best fit value for the NP contribution $\Delta C_7^{\rm eff} = C_7^{\rm eff}(m_b) - C_{7\rm SM}^{\rm eff}(m_b)$ is very close to the SM point residing in the origin, while the wrong-sign solution located on the right is highly disfavored, as it corresponds to a $\mathrm{BR}(\bar{B} \to X_s\ell^+\ell^-)$ value considerably higher than the measurements [44]. The corresponding limits are [40]

$$\Delta C_7^{\rm eff} = -0.039 \pm 0.043 \;\; (68\%\,\mathrm{CL})\,, \quad \Delta C_7^{\rm eff} = [-0.104, 0.026] \cup [0.890, 0.968] \;\; (95\%\,\mathrm{CL})\,. \quad (4.2)$$

Similar bounds have been presented previously in [39]. Since $\mathrm{BR}(\bar{B} \to X_s\gamma)_{\rm SM}$ as given in Eq. (3.1) is lower than the experimental world average $\mathrm{BR}(\bar{B} \to X_s\gamma) = (3.55 \pm 0.26) \times 10^{-4}$ [45] by $1.2\,\sigma$, extensions of the SM that predict a suppression of the $b \to s\gamma$ amplitude are strongly constrained. In particular, even the SM point $\Delta C_7^{\rm eff} = 0$ is almost disfavored at 68% CL by the global fit.

The stringent bound on the NP contribution ΔC given in Eq. (4.1) translates into tight two-sided limits for the BRs of all Z-penguin dominated K- and B-decays [40]. In the case of the $K \to \pi\nu\bar{\nu}$ modes the allowed ranges for the CMFV BRs read [40]

$$\begin{aligned} \mathrm{BR}(K_L \to \pi^0\nu\bar{\nu})_{\rm CMFV} &= [1.55, 4.38] \times 10^{-11} \quad (95\%\,\mathrm{CL})\,, \\ \mathrm{BR}(K^+ \to \pi^+\nu\bar{\nu}(\gamma))_{\rm CMFV} &= [4.29, 10.72] \times 10^{-11} \quad (95\%\,\mathrm{CL})\,, \end{aligned} \quad (4.3)$$

when NP contributions to EW boxes are neglected. These bounds imply that in CMFV models the $K_L \to \pi^0\nu\bar{\nu}$ and $K^+ \to \pi^+\nu\bar{\nu}(\gamma)$ rates can differ by at most $^{+18\%}_{-21\%}$ and $^{+27\%}_{-30\%}$ from their SM expectations. In particular, the Grossman-Nir bound $\mathrm{BR}(K_L \to \pi^0\nu\bar{\nu}) \lesssim 4.4\,\mathrm{BR}(K^+ \to \pi^+\nu\bar{\nu}(\gamma))$

[46] following from isospin symmetry, cannot be saturated in CMFV models. This is illustrated by the plot in the right panel of Fig. 4 which shows the frequentist $1-\mathrm{CL}$ level of the prediction $\mathrm{BR}(K^+ \to \pi^+ \nu\bar{\nu}(\gamma))_{\mathrm{CMFV}}$ *vs.* $\mathrm{BR}(K_L \to \pi^0 \nu\bar{\nu})_{\mathrm{CMFV}}$.

A strong violation of the CMFV bounds in Eq. (4.3) by future precision measurements of $\mathrm{BR}(K_L \to \pi^0 \nu\bar{\nu})$ and/or $\mathrm{BR}(K^+ \to \pi^+ \nu\bar{\nu}(\gamma))$ will imply a failure of the CMFV assumption, signaling either the presence of new effective operators and/or new flavor and *CP* violation. A way to evade the above limits is the presence of sizable EW box contributions. While these possibility cannot be fully excluded, general arguments and explicit calculations indicate that it is difficult to realize in the CMFV framework.

References

[1] C. Tarantino, these proceedings and 0706.3436 [hep-ph]; C. Smith, these proceedings; 0707.2309 [hep-ph] and references therein.

[2] M. Misiak and J. Urban, Phys. Lett. B **451**, 161 (1999); G. Buchalla and A. J. Buras, Nucl. Phys. B **548**, 309 (1999).

[3] G. Buchalla and A. J. Buras, Phys. Rev. D **57**, 216 (1998).

[4] W. J. Marciano and Z. Parsa, Phys. Rev. D **53**, 1 (1996).

[5] F. Mescia and C. Smith, Phys. Rev. D **76**, 034017 (2007).

[6] A. J. Buras *et al.*, Phys. Rev. Lett. **95**, 261805 (2005) and JHEP **0611**, 002 (2006).

[7] A. F. Falk, A. Lewandowski and A. A. Petrov, Phys. Lett. B **505**, 107 (2001).

[8] G. Isidori, F. Mescia and C. Smith, Nucl. Phys. B **718**, 319 (2005).

[9] G. Isidori, G. Martinelli and P. Turchetti, Phys. Lett. B **633**, 75 (2006).

[10] J. Charles *et al.* [CKMfitter Group], Eur. Phys. J. C **41**, 1 (2005) and updated results and plots available at http://ckmfitter.in2p3.fr

[11] M. Misiak and M. Steinhauser, Nucl. Phys. B **683**, 277 (2004); M. Gorbahn and U. Haisch, Nucl. Phys. B **713**, 291 (2005); M. Gorbahn, U. Haisch and M. Misiak, Phys. Rev. Lett. **95**, 102004 (2005). K. Melnikov and A. Mitov, Phys. Lett. B **620**, 69 (2005); I. Blokland *et al.*, Phys. Rev. D **72**, 033014 (2005); H. M. Asatrian *et al.*, Nucl. Phys. B **749**, 325 (2006); B **762**, 212 (2007) and Phys. Lett. B **647**, 173 (2007); M. Czakon, U. Haisch and M. Misiak, JHEP **0703**, 008 (2007).

[12] K. Bieri, C. Greub and M. Steinhauser, Phys. Rev. D **67**, 114019 (2003); R. Boughezal, M. Czakon and T. Schutzmeier, 0707.3090 [hep-ph].

[13] M. Misiak and M. Steinhauser, Nucl. Phys. B **764**, 62 (2007).

[14] M. Misiak *et al.*, Phys. Rev. Lett. **98**, 022002 (2007).

[15] P. Gambino and M. Misiak, Nucl. Phys. B **611**, 338 (2001).

[16] A. J. Buras *et al.*, Nucl. Phys. B **631**, 219 (2002) and references therein.

[17] A. Kapustin, Z. Ligeti and H. D. Politzer, Phys. Lett. B **357**, 653 (1995).

[18] Z. Ligeti, L. Randall and M. B. Wise, Phys. Lett. B **402**, 178 (1997); G. Buchalla, G. Isidori and S. J. Rey, Nucl. Phys. B **511**, 594 (1998).

[19] S. J. Lee, M. Neubert and G. Paz, Phys. Rev. D **75**, 114005 (2007).

[20] M. Neubert, Phys. Rev. D **49**, 4623 (1994); I. I. Y. Bigi *et al*., Int. J. Mod. Phys. A **9**, 2467 (1994).

[21] M. Neubert, Eur. Phys. J. C **40**, 165 (2005).

[22] T. Becher and M. Neubert, Phys. Rev. Lett. **98**, 022003 (2007).

[23] M. Misiak, private communications (2007).

[24] A. Vogt, Phys. Lett. B **497**, 228 (2001); T. Becher and M. Neubert, Phys. Lett. B **637**, 251 (2006).

[25] G. P. Korchemsky and A. V. Radyushkin, Nucl. Phys. B **283**, 342 (1987); I. A. Korchemskaya and G. P. Korchemsky, Phys. Lett. B **287**, 169 (1992); G. P. Korchemsky and G. Marchesini, Nucl. Phys. B **406**, 225 (1993); E. Gardi, JHEP **0502**, 053 (2005); T. Becher and M. Neubert, Phys. Lett. B **633**, 739 (2006).

[26] J. R. Andersen and E. Gardi, JHEP **0701**, 029 (2007); E. Gardi, hep-ph/0703036.

[27] E. Gardi, hep-ph/0606080 and references therein.

[28] E. Gardi, private communications (2007).

[29] A. Ghinculov *et al*., Nucl. Phys. B **685**, 351 (2004).

[30] C. Bobeth *et al*., JHEP **0404**, 071 (2004).

[31] T. Huber *et al*., Nucl. Phys. B **740**, 105 (2006).

[32] Z. Ligeti and F. J. Tackmann, 0707.1694 [hep-ph].

[33] C. Bobeth, M. Misiak and J. Urban, Nucl. Phys. B **574**, 291 (2000); H. H. Asatryan *et al*., Phys. Lett. B **507**, 162 (2001); Phys. Rev. D **65**, 074004 (2002) and D **66**, 034009 (2002); H. M. Asatrian *et al*., Phys. Rev. D **66**, 094013 (2002); A. Ghinculov *et al*., Nucl. Phys. B **648**, 254 (2003); P. Gambino, M. Gorbahn and U. Haisch, Nucl. Phys. B **673**, 238 (2003).

[34] K. S. M. Lee and I. W. Stewart, Phys. Rev. D **74**, 014005 (2006); K. S. M. Lee *et al*., Phys. Rev. D **74**, 011501 (2006);

[35] B. Aubert *et al*. [BaBar Collaboration], Phys. Rev. Lett. **93**, 081802 (2004); K. Abe *et al*. [Belle Collaboration], hep-ex/0408119.

[36] K. S. M. Lee *et al*., Phys. Rev. D **75**, 034016 (2007).

[37] G. D'Ambrosio *et al*., Nucl. Phys. B **645**, 155 (2002); G. Hiller and F. Krüger, Phys. Rev. D **69**, 074020 (2004); P. J. Fox *et al*., 0704.1482 [hep-ph]; M. Bona *et al*. [UTfit Collaboration], 0707.0636 [hep-ph].

[38] A. Ali *et al*., Phys. Rev. D **66**, 034002 (2002).

[39] C. Bobeth *et al*., Nucl. Phys. B **726**, 252 (2005).

[40] U. Haisch and A. Weiler, 0706.2054 [hep-ph], to appear in Phys. Rev. D.

[41] M. Blanke *et al*., JHEP **0610**, 003 (2006).

[42] S. Schael *et al*. [ALEPH Collaboration], Phys. Rept. **427**, 257 (2006).

[43] S. Chen *et al*. [CLEO Collaboration], Phys. Rev. Lett. **87**, 251807 (2001); P. Koppenburg *et al*. [Belle Collaboration], Phys. Rev. Lett. **93**, 061803 (2004); B. Aubert *et al*. [BaBar Collaboration], Phys. Rev. Lett. **97**, 171803 (2006).

[44] P. Gambino, U. Haisch and M. Misiak, Phys. Rev. Lett. **94**, 061803 (2005).

[45] E. Barberio *et al*. [Heavy Flavor Averaging Group], 0704.3575 [hep-ex] and online update available at http://www.slac.stanford.edu/xorg/hfag

[46] Y. Grossman and Y. Nir, Phys. Lett. B **398**, 163 (1997).